Power law dependence found on the lifetime of a photoconductor chaotic transient numerically induced by a fixed-step algorithm

Alicia Serfaty de Markus
Centro de Estudios Avanzados en Optica, Facultad de Ciencias, Universidad de los Andes, Mérida, Venezuela
(Received 5 August 1996)

A direct procedure is proposed to determine whether a chaotic transient is caused by the dynamic of a system or by the numerical artifact employed to solve it. This test is carried out by correlating the resulting lifetimes of the chaotic transients for independent driving parameters of a nonlinear system. In this work the transient behavior of a photoconductor model was investigated for two different parameters such as the capture probability and the trap density. The model was integrated with a conventional fixed-step Runge-Kutta technique, displaying a complex intermittent transient that breaks down through bifurcation reversals into the fixed points of the system. It was found that the corresponding average escape time of these transients follows a power law dependence with the driving parameter, in accordance with the theories of Grebogi, Ott, and York. However, for the two physically independent parameters involved, the average lifetime yielded exactly the same critical exponent. These results directly imply the role of the algorithm as the common underlying source where the chaotic transients are numerically induced, in complete agreement with previous studies on this system. [S1063-651X(97)13401-8]

PACS number(s): 05.45.+b, 05.40.+j, 02.70.−c, 72.40.+w

INTRODUCTION

For the vast majority of nonlinear systems, dynamical studies have to be performed with the help of numerical resources, insofar as only the simpler models have analytical solution, and, even so, it is far easier to employ numerical techniques. The trade-off, however, arises when the numerical results not only differ but even interfere with the ''real'' results. In particular, the proper choice of a numerical method becomes relevant when the dynamics becomes chaotic. This aspect has been discussed extensively in Ref. [1], where the effect of the numerical integration of some nonlinear test models was manifested as spurious asymptotic states. Or, as in the case of a nonlinear photoconductor model recently studied [2], the outcome of the numerical integration had its impact over the transient response in the form of an intermittent chaotic transient. Due to complex dynamics that could result from an increasingly complicated nonlinear system, there is no distinctive line capable of delimiting a truly chaotic behavior from that emerging out of the numerics. In fact, both situations could be intricately interwoven.

The present work investigates the effect upon the escape time of the chaotic transient as two physically independent photoconductor parameters are independently varied, with the purpose of determining up to what extent the resulting escape time parameter dependence may disagree with a power law relation expected for a chaotic transient [3] as a result of the integration numerical artifact.

EXPERIMENTAL METHOD

The photoconductor model consists of three coupled nonlinear ordinary differential equations describing the population densities of electrons n, trapped electrons m, and holes p, given, respectively, as [4]

$$\frac{dn}{dt} = G - n\alpha_1(N_t - m) + \beta m - c_1 n,$$

$$\frac{dm}{dt} = n\alpha_1(N_t - m) - \delta_0 mp - \beta m, \tag{1}$$

$$\frac{dp}{dt} = G - \delta_0 mp - c_2 p.$$

In short, system (1) describes the photoconducting process in a semiconductor with one type of trap level, which is located near the conduction band as to ensure a significative reemission of the trapped electrons back to this band. Free electrons are trapped with a probability α_1 into the trap level, at a rate proportional to the sites available at that level, given as the factor $n\alpha_1(N_t - m)$, where N_t is the trap density. Thus the trapped electron population m increases at a rate proportional to the same factor, such that there is an inverse relationship between α_1 and N_t as to keep the same population rates. A more detailed description of the physical meaning of the other parameters is given in Ref. [5].

It was found that there is a critical set of parameters for which the photoconductor system (1) is locally unstable according to its eigenvalues [6], and displays chaotic behavior and numerical overflow. However, as a result of the stiffness produced by these parameters over the system, it was found in Ref. [2] that a conventional fixed step Runge-Kutta integration algorithm could induce this chaotic behavior, as it completely disappears when integrated with a variable step integrator, such as the Gear method and the Adams-Moulton integrators. These parameters values are $G = 10^{16}$ electron-hole pairs/cm^2 s, $c_1 = 1.5\times10^{-3}$ s^{-1}, $c_2 = 1.5\times10^{-5}$ s^{-1}, $\delta_0 = 10^{-15}$ cm^{-3} s^{-1}, and $\beta = 0.83$ s^{-1}. In this study, the trap density N_t and the capture probability α_1 are to be varied as 10^6 cm$^{-3} < N_t < 4.85\times10^{15}$ cm^{-3} and 2.5×10^{-15} cm^{-3} s$^{-1} < \alpha_1 < 4.641\times10^{-14}$ cm^{-3} s^{-1}, respectively.

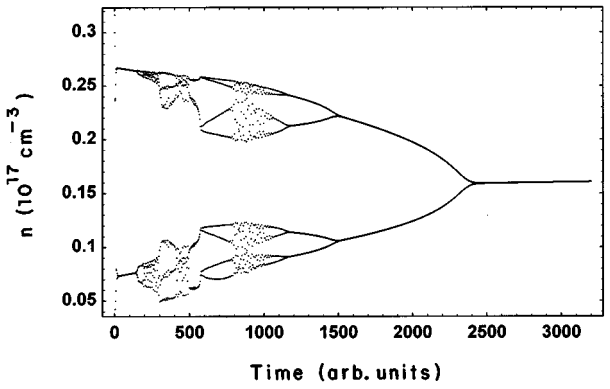

FIG. 1. Transient response of the free electrons for $\alpha_1=2.5\times10^{-15}$ cm^{-3} s^{-1} and $N_t=8\times10^{14}$ cm^{-3} obtained with the RK algorithm for a step size $s=0.05$.

Figure 1 shows a typical transient response for the electron population for $N_t=8\times10^{14}$ cm^{-3}, and $\alpha_1=2.5\times10^{-15}$ cm^{-3} s^{-15} when integrated with the Runge-Kutta method for a step size $s=0.05$. The intermittent chaotic structure and the breakdown by reverse bifurcations of the time series is revealed in Fig. 1, when omitting the lines joining the successive points generated by the numerical outcome. The escape time t_e is taken as the average time in which the transient just enters a nonoscillatory state, going from the beginning at $t=0$ through the stages of chaotic intermittence and reverse bifurcations to the very moment that the transient reaches a period-1 oscillation. A similar behavior is displayed for the trapped electrons and holes, as depicted in Fig. 2 showing a parametric three-dimensional plot of n, m, and p. Chaotic transients obtained through integration with smaller step sizes yields a much more dense attractor (as a matter of fact a ''repeller,'' since the orbits eventually escape that structure following the straight line shown in Fig. 2).

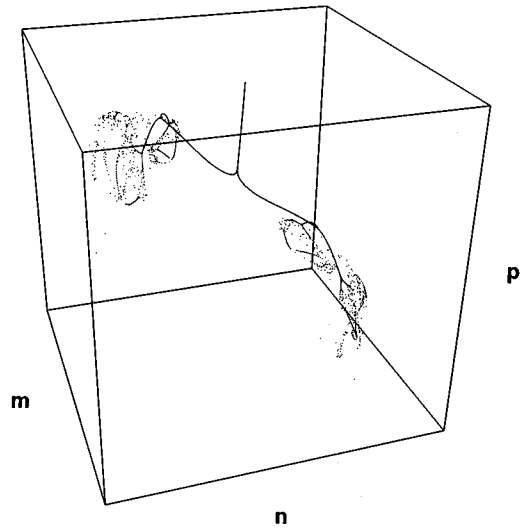

FIG. 2. Repeller found in phase space for $\alpha_1=2.5\times10^{-15}$ cm^{-3} s^{-1} and $N_t=8\times10^{14}$ cm^{-3} for the RK algorithm with $s=0.05$. After a finite time, the orbits falls into the system fixed point attractor through the straight line shown.

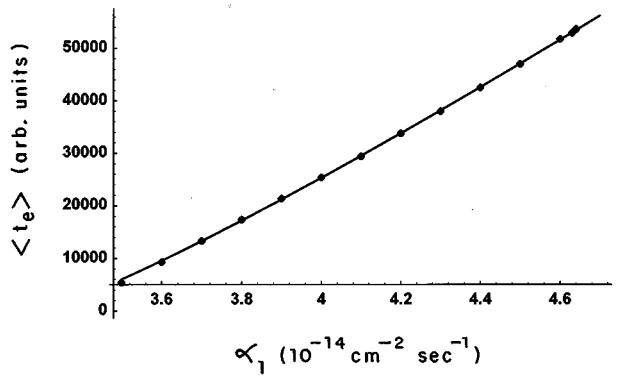

FIG. 3. Average escape time of the chaotic transients with the capture probability as the driving parameter. The dotted line corresponds to the numerical results according to the RK algorithm with step size $s=0.01$. The continuous line is for a power law least-squares fit to data with exponent $\gamma=1.15$.

RESULTS AND DISCUSSION

The average escape time obtained for 3.5×10^{-14} cm^{-3} s$^{-1}\leqslant\alpha_1\leqslant4.641\times10^{-14}$ cm^{-3} s^{-1} was plotted as the dotted line of Fig. 3. Numerical integration was carried out for a step size of $s=0.01$, for which, beyond $\alpha_1=4.641\times10^{-14}$ cm^{-3} s^{-1}, the system enters numerical overflow. Despite the appreciable linear trend followed by the escape time, a better fit to data is achieved by a power law dependence rather than by a straight line, in agreement with the theories of Grebogi, Ott, and Yorke [3]. The continuous line in Fig. 3 is an excellent fit by least squares, corresponding to

$$\langle t_e\rangle=K_1(\alpha_1-\alpha_c)^{\gamma_1}, \tag{2}$$

where $\alpha_c=3.3\times10^{-14}$ cm^{-3} s^{-1} is the critical parameter, $\gamma_1=1.15$ is the critical exponent for the chaotic transient, and $K_1=38\,156.9$ is a fitting parameter. Although this critical exponent is close to 1, a definite power law dependence is present, as slight changes of γ_1 produce appreciable alterations in the solid curve of Fig. 3. Accordingly, the corresponding log-log plot shown in Fig. 4 is close to a straight line; the small but noticeable curvature present in Fig. 4 indicates not a deviation from a simple type of power law (2) but instead the contribution of at least two power-dependent

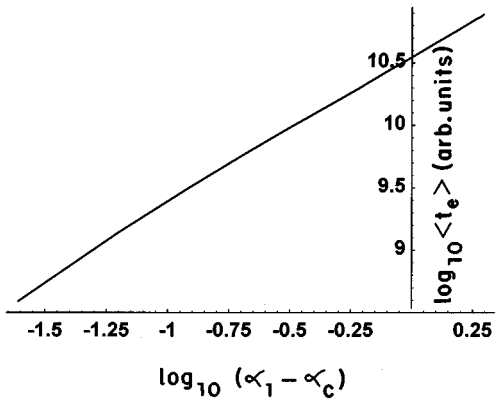

FIG. 4. Log-log plot of the average escape time with the capture probability showing a power law dependence.

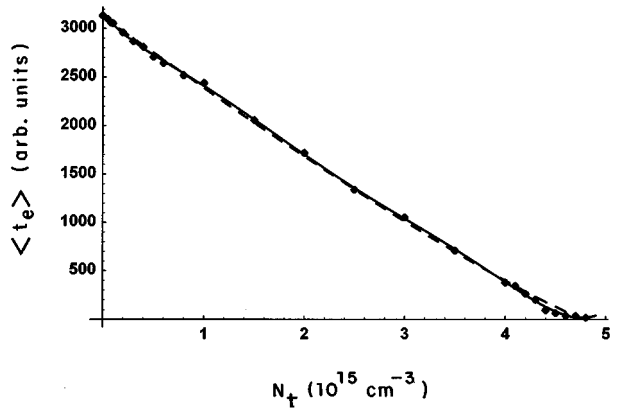

FIG. 5. Average escape time of the chaotic transients with the trap density as the driving parameter. The dotted line corresponds to the numerical results according to the RK algorithm with step size $s=0.05$. The continuous line corresponds to a power series fit to data. The dashed line is for a simple power law fit to data with exponent $\gamma=1.15$.

terms. A similar situation was reported in experimental measurements of chaotic transients detected in a ferromagnetic material under dc and rf magnetic fields [7], where deviation of a simple power law was found for those chaotic transients where intermittent behavior was present. For the photoconductor system (1), the chaotic transients were all intermittent.

In Fig. 5, a plot of the average escape time versus the density of traps is represented as a dotted line for 10^6 cm$^{-3}\leqslant N_t\leqslant 5\times10^{15}$ cm^{-3}. In this case, the Runge-Kutta integration was done for a step size equal to 0.05. It was found that for 10^6 cm$^{-3}<N_t<8\times10^{12}$ cm^{-3}, the escape time remains constant ($t_c=3135$ a.u.), decreasing afterwards as N_t approaches 4.85×10^{15} cm^{-3}. The system transient behavior is chaotic for $N_t<3\times10^{15}$ cm^{-3}, and quasiperiodic for higher impurities concentrations. For $N_t>4.85\times10^{15}$ cm^{-3} the photoconductor becomes unstable, as a further increase beyond this value produces numerical overflow. It was found that the best fit to data was met for a sixth-order power series, indicated by the continuous line of Fig. 5. The dashed line represents the next best fit to data according to a power law dependence, and is given as

$$\langle t_e\rangle = K_2(N_c-N_t)^{\gamma_2}, \tag{3}$$

with $N_c=4.8\times10^{15}$ cm^{-3} being the critical parameter, $\gamma_2=1.15$ the critical exponent, and $K_2=514$ a fitting parameter. Although small, the deviation for the power law fit (3) is possibly related to a reduced numerical resolution resulting from the larger step size employed. Thus there is a more pronounced scattering of the data, in particular at the high impurity region where the system became unstable; see Fig. 5. As before, the corresponding log-log plot deviates from the simple power law dependence (3). Nevertheless, it is remarkable that the average escape time for the trap density approaches the same critical exponent $\gamma=1.15$, already found for the capture probability.

The fact that for variations of both α_1 and N_t the critical exponents γ are the same, strongly suggests that the chaotic transients are being caused by the numerical algorithm, and not by the intrinsic dynamic of the photoconductor system, in agreement with our previous study [2]. On the other hand, since the capture probability and trap density are related in our model in an unique way, we should consider, fundamentally, the physical relation between these parameters. In addition, it should also be included that numerical considerations regarding the observed overflow emerge from the unstable photoconductor.

This could be the case if, for a given set of parameters, the system becomes unstable and/or stiff [2,6]. For a fixed-step integration routine such as the Runge-Kutta algorithm employed here, numerical overflow occurs when initially small errors propagate through the integration and become unbounded. Reducing the step size could overcome this problem [2], but it makes an otherwise efficient algorithm computationally inefficient. With a self-adjusting routine such as the Gear scheme [8], the number of integration steps are minimized, and, thus, it is possible to reduce the computation time and the accumulated round-off error, while meeting stability considerations. Most important, as a direct consequence, a self-adjusting step-order routine improves numerical stability, as the region of stability of the algorithm is comparatively larger with respect to the stability region of fixed-step explicit algorithms such as the Runge-Kutta (RK) scheme. Such stability regions are representations of the stability of a given method standardized through the integration of the test equation $y'=\lambda y$. Here an algorithm will be stable if any single error made in applying the method will have an effect such that the results still imitates the exact solution. This implies certain constraints for the values of the step size and the time constants, that can be represented as regions in the complex plane in terms of the factor $h\lambda$ [8]. Then, for a given set of parameters, the resulting time constants may severely limit the size of the integration step, in order to keep the $h\lambda$ factor inside the stability region of a given algorithm. Otherwise, the small errors will be magnified exponentially, resulting in numerical overflow. This situation was observed when integrating the photoconductor equations (1) with the RK scheme, and avoided when employing implicit routines such as the Gear and Adam-Moulton schemes [2].

This behavior is particularly relevant for rigid systems with its disparate time scales, such as the present one. Although for the first order test equation the eigenvalue λ is simply related to the time constant as $-1/\lambda$, for the more complicated nonlinear systems the time constants are not so obvious. Nevertheless, an estimation of the time scales could be accomplished through the system eigenvalues, with the Jacobian evaluated at several points [6].

From a physical perspective, the photoconductor dynamics could become very complex due to the various competitive processes involved. The kinetics of the charge carriers is controlled by processes of generation, trapping, and recombination, as expressed through the nonlinear rate equations (1). These equations include feedback between the electrons from the conduction band and the traps. In particular, the instability of the system is expected, as the role of the traps becomes predominant. The interplay between the conduction band and the traps is enhanced, and becomes significant as the traps are filled. This situation is achieved in several ways, two of which are considered here in particular. One is to increase the capture probability. The other is to reduce the

number of sites available in the traps by simply keeping a low trap density for a relatively high generation rate and a given capture probability.

In fact, chaotic transients were consistently observed when the capture probability was increased [2] or when the trap density was decreased (see Fig. 1), while keeping the rest of the parameters fixed. Thus the origin of the transient could be directly related to the number of sites available at the trap level, which, in turn, is related to a strong interaction between trap density and capture probability. Conversely, as the trap density increases, this interplay is not so predominant, as the number of available sites rises and no chaotic transient is observed so far; however, as the population of the impurities increases, the photoconductor becomes unstable, as physically expected; thus a numerical scheme such as the one employed in this study may become unstable, especially if integrating over a stiff system. In short, while for the capture probability α_1 the route to overflow coincides with an increasingly chaotic transient, as reported in Ref. [2], the opposite was found for the trap densities N_t. Therefore, these results might be interpreted as if there are physical situations capable of inducing a type of unstability over the (fixed step) numerical algorithm different from those producing plain overflow. Both physical and numerical factors affect the stability of the system in a similar manner and, hence, separation of the origin becomes a crucial task.

From a numerical perspective, the photoconductor stability could be determined examining the system eigenvalues [6] (just the real part, as the imaginary part is negligibly small). The t_e (N_t) behavior shown in Fig. 5 coincides with appreciable changes (in magnitude) for the system eigenvalues: as N_t increases, one of the eigenvalues increases steadily, another eigenvalue decreases very fast, and the remaining eigenvalue changes moderately for the range studied (λ_1: $-0.000\,75 \rightarrow -11.26$, λ_2: $-833\,323 \rightarrow -89.75$, and λ_3: $-0.000\,75 \rightarrow -0.000\,015$ for 10^6 cm$^{-3} < N_t < 4.8\times10^{15}$ cm^{-3}). As N_t approaches and passes the breakpoint where overflow was observed ($N_t \geqslant 4.85\times10^{15}$ cm^{-3} for $s=0.05$), there is a notorious change in the eigenvalues (magnitude) behavior: the rate of increase for the first eigenvalue is enhanced, and the magnitude of the other eigenvalue reverses from decreasing to a great increase (λ_1: $-11.72 \rightarrow -116.78$, λ_2: $-86.2 \rightarrow -124\,709$, λ_3: $-0.000\,015 \rightarrow -2.07\times10^{-8}$ for 5×10^{15} cm$^{-3} < N_t < 5\times10^{19}$ cm^{-3}; this upper limit corresponds to a degenerated semiconductor). These variations may induce an algorithm to become unstable, and thus to overflow, since the region of stability of a given algorithm is greatly dependent on the inverse relationship of the step size s and the eigenvalue λ [8]. That explains why reducing the step size was enough for the overflow to disappear. A similar relationship between the eigenvalues and the numerical overflow has been reported for the capture probability α_1 in Ref. [2], with the onset of the overflow coincidentally happening in the direction where the lifetime of the chaotic transient increases.

Like the time series reported in Ref. [2] for changes in the capture probability, those obtained for changes in the trap densities (see Fig. 1) were chaotic according to their sensitivity to initial conditions, their broad power spectrum, a characteristic return map for the variables, and the emergence of an attractor in phase space (see Fig. 2); these tools are part of the standard procedures usually applied (as a parameter is varied) when searching for chaotic dynamics. In particular, there is a great similitude between the time series of Fig. 1 and a variety of structures reported in the literature: in the Belousov-Zhabotinsky-simulated chemical reaction as a function of the flow rate [9]; in a model involving perturbation of the respiratory system with the phase of the stimuli cycle as the bifurcation parameter [10]; in experimental chaotic heart dysrhytmias as a function of the pacing cycle lengths [11]; and other ''antimonotonic'' structures showing bifurcation reversals [12]. However, it is worth emphasizing that the most striking feature here is that the photoconductor chaotic patterns and bifurcation reversals are found directly in the time series. Such a behavior was reported in Ref. [2], where it was proposed and discussed that the deterministic nonlinear iterative rules specific of the fixed-step Runge-Kutta algorithm were responsible for these chaotic transients. Therefore, as time progresses, it is not in the space parameter where these chaotic structures are to be found. The most direct proof that this dynamic is caused by the algorithm was given when an adaptive algorithm was employed; here, regardless of the parameters values, we observed neither overflow nor chaos when integrating with a variable step-order method [13].

Now, focusing on the time series, a chaotic transient should display a power law dependence according to the numerical studies of Grebogi, Ott, and Yorke [3]. Their theory states that a chaotic transient occurs when a stable chaotic attractor becomes unstable, and is destroyed when colliding with the boundary of attraction of a nonchaotic attractor at some critical value of the driving parameter. This type of event, in which the formerly chaotic attractor is destroyed, is called a boundary crisis, and the escape time t_e is the finite time spent by trajectories initialized in the region of the destroyed chaotic attractor moving around its neighborhood before escaping to a stable nonchaotic attractor. The average duration $\langle t_e \rangle$ of the chaotic transient is given as $\langle t_e \rangle = (p - p_c)^{\gamma}$, with γ the critical exponent and p_c the critical parameter at which the collision occurs. Thus, in a boundary crisis, for parameter values just past the crisis point, the attractor no longer exists, and the trajectories appear to move chaotically, like before the crisis occurred, but only for a finite time. This law has been numerically and experimentally verified in several cases [14].

In the present work, results for the escape time with the capture probability and the trap densities as the driving parameters [Eqs. (2) and (3), respectively] are in close agreement with a power law dependence predicted by theories of Ref. [3]. For the capture probability, the chaotic transient was observed for values of the parameter past $\alpha_1 = 3.5\times10^{-14}$ cm^{-3} s^{-1}, which is in good agreement with the value found for the critical parameter $\alpha_c = 3.3\times10^{-14}$ cm^{-3} s^{-1} in Eq. (2). However, the transient behavior for the trap parameter deserves a closer look.

With the trap density as the driving parameter, chaotic transients were observed *up to* $N_t < 3\times10^{15}$ cm^{-3}; for higher values the system falls into a nonchaotic attractor. The value found for the critical parameter was $N_c = 4.8\times10^{15}$ cm^{-3}, which is very close to the breakpoint of the onset of overflow, $N_t \geqslant 4.85\times10^{15}$ cm^{-3}. Following the ideas of Grebogi, Ott, and Yorke [3], the critical parameter for this case should

be expected around $N_c=3\times10^{15}$ cm^{-3}, where the onset of chaotic transients was observed with the N_t parameter decreasing [thus, in Eq. (3), the corresponding critical parameter N_c appears to be subtracted from the driving parameter N_t, rather than the opposite as in Eq. (2)]. Thus it could be considered a subset of the escape time data for the range of N_t where all transients were strictly chaotic, as for the α_1 case of Fig. 4; nevertheless, it was found that for these selected points a fit with the power law of Eq. (3) with $N_c=3\times10^{15}$ cm^{-3} (and $\gamma_2=1.15$) gives a great deviation. Conversely, keeping $N_c=4.8\times10^{15}$ cm^{-3} as before gives a close fit, especially in the lower impurity region. Therefore, there is no critical parameter N_c that just passes by to unfold a boundary crisis and thus a truly chaotic transient, despite the fact that a truly chaotic ''object'' is actually seen in the time series. This in turn directly implies that if there is a combination of parameters causing the system to become unstable and to overflow numerically in one extreme of the curve of Fig. 5, there is another combination of parameters *numerically* responsible for the chaotic behavior at the other end of this unique curve. In fact, such a chaos-producing alliance of parameters is given (specifically α_1 and N_t), as they physically merge into one common factor: the available sites at the trap level. In consequence, those considerations regarding the $t_e(N_t)$ behavior of Eq. (3) must hold true for the $t_e(\alpha_1)$ behavior of Eq. (2); it now becomes apparent why both expressions share the same critical exponent, as both are linked to the same underlying numerical artifact.

CONCLUSION

The average lifetime of the chaotic transients found in a photoconductor system with one trap level was examined separately as a function of the capture probability and the trap density. The escape time yielded a power law dependence for each driving parameter, as expected for chaotic transients, but with exactly the same critical exponent. This parallelism is considered direct evidence that the integration algorithm produces the chaotic transient and, thus, that the escape time reflects this unique source. These results are in agreement with a previous study of the photoconductor model [2], where simply changing the numerical integration technique revealed an algorithm induction of chaos. For more complex systems, where such a strategy may not lead to similar direct results, examining the degree of correlation between the escape times for two or more independent parameters could be a value and even easier option in detecting numerically created chaos.

ACKNOWLEDGMENTS

The author wants to thank Dr. N. V. Joshi for useful discussion. This work was supported by the Consejo de Desarrollo Científico de la Universidad de los Andes under Project No. C-621-93A.

[1] H. C. Yee, P. K. Sweby, and D. F. Griffiths, J. Comput. Phys. **97**, 249 (1991).
[2] A. Serfaty de Markus (unpublished), and in *Proceedings of the Numerical Methods in Engineering Simulation* (Computational Mechanics, Southampton, 1996), pp. 249–255.
[3] C. Grebogi, E. Ott, and J. Yorke, Physica **7D**, 181 (1983).
[4] N. V. Joshi, in *Photoconductivity: Art, Science and Technology* (Marcel Dekker, New York, 1990).
[5] A. Serfaty and N. V. Joshi, Phys. Rev. B **47**, 3983 (1993).
[6] A. Serfaty de Markus and N. V. Joshi, Chaos Solitons Fractals **7**, 1095 (1996).
[7] T. L. Carroll, L. M. Pecora, and F. J. Rachford, Phys. Rev. A **40**, 377 (1989).
[8] T. S. Parker and L. O. Chua, *Practical Numerical Algorithms for Chaotic Systems* (Springer-Verlag, New York, 1989).
[9] L. Györgyi and R. Field, Nature **355**, 808 (1992).
[10] J. Lewis, M. Bachoo, L. Glass, and C. Polosa, Phys. Lett. A **125**, 119 (1987).
[11] D. Chialvo, R. Gilmour, and J. Jalife, Nature **343**, 653 (1990).
[12] S. P. Dawson, C. Grebogi, J. A. Yorke, I. Kan, and H. Kocak, Phys. Lett. A **162**, 249 (1992).
[13] C. W. Gear, *Numerical Initial Value Problems in Ordinary Differential Equations* (Prentice-Hall, Englewood Cliffs, NJ, 1971).
[14] T. Tèl, in *Transient Chaos, Directions in Chaos*, edited by Hao Bai-Lin (World Scientific, Singapore, 1990), Vol. 3, pp. 149–211.